Catalysis Today 166 (2011) 60–66

Contents lists available at ScienceDirect

Catalysis Today

journal homepage: www.elsevier.com/locate/cattod

Characterization and catalytic evaluation of aluminum oxides obtained by the atrane route

Gustavo García[b], Marisa Falco[a], Pedro Crespo[b], Saúl Cabrera[b], Ulises Sedran[a,*]

[a] Instituto de Investigaciones en Catálisis y Petroquímica INCAPE (FIQ, UNL - CONICET), Santiago del Estero 2654, 3000 Santa Fe, Argentina
[b] Laboratorio de Sólidos y Química Teórica, Instituto de Investigaciones Químicas (I.I.Q.), Universidad Mayor de San Andrés, Campus Universitario, Cota Cota Calle N° 27, La Paz, Bolivia

ARTICLE INFO

Article history:
Available online 15 September 2010

Keywords:
Alumina
Atrane
Catalytic cracking

ABSTRACT

The atrane route (aluminum tri-sec butoxide as the metal source mixed with tri-ethanolamine to yield the alumatrane complex) was used to synthesize aluminas that showed specific surface areas in the 150–275 m^2/g range and average pore sizes in the 60–180 Å range after calcination. Different techniques were used to characterize the aluminas (IR, XRD, ^{27}Al MAS-NMR, N_2 adsorption). The amount of organic matter trapped in the inorganic matrix in the uncalcined materials decreased as a function of the increasing molar relationship between water and the atrane complex in the synthesis, which ranged from 9 to 78. Crystalline micro domains of the γ-AlOOH boehmite-type were formed in the uncalcined samples that increased their size as a function of the proportion of water in the synthesis, because water favors the hydrolysis and condensation of the $Al[N(CH_2–CH_2–O)_3]_2H_3$ complex. The calcination treatment induced the crystalline restructuration from boehmite-type to γ-alumina-type structures. Thus, the calcined mesoporous aluminas showed an amorphous structure, with crystal micro domains of γ-alumina-type that also increased their size as a function of the amount of water in the starting mixtures. As compared to the properties of a sample prepared by the conventional sol–gel method, the moderate hydrothermal treatment in the atrane synthesis route favored the release of trapped organic matter and the formation of initial boehmite-type micro domains; specific surface areas were similar, but the pore size distributions were sharper in the materials prepared with the atrane route. The activities of the aluminas prepared by the atrane route, as indicated by the TIPB conversion at 500 °C and short reaction times from 12 to 30 s in a CREC Riser Simulator laboratory reactor, were somewhat smaller than those observed in conventional aluminas. The apparent kinetic parameters in a simple, first order model were similar, suggesting that accessibility limitations from the pore systems were not present. The properties shown by these aluminas synthesized by the atrane route indicated a preliminary appropriate condition for being used as FCC catalyst matrices.

1. Introduction

The particular characteristics of aluminum oxides, such as specific surface area, acidic properties, and resistance to severe hydrothermal conditions, among others, sustain their use as catalyst supports or matrices, and lead to an increase in the associated research efforts [1]. Commercial adsorption and catalysis applications use transition aluminas (γ- or η-alumina) derived from the thermal treatment of aluminum tri-hydroxide such as gibbsite or from aluminum oxy-hydroxides such as boehmite gels [2]. These applications are usually operated under severe conditions, such as high temperatures and pressures. The technology associated with these conditions requires other properties from aluminas, such as mechanical strength and adequate particle shape and size. Alumina precursors such as boehmite gels offer good properties for agglomeration and shaping with conventional techniques (extrusion, bead forming or pelletization); as a result, alumina hydrates are commonly used as binders to agglomerate other solids such as zeolites [1]. Lesaint et al. [3] described the synthesis and characterization of new alumina materials prepared in the presence of anionic, cationic and non-ionic surfactants. They adopted a double hydrolysis strategy by using Al^{3+} and AlO^{2-} ions in successive steps, obtaining materials with relatively high surface area, narrow pore size distribution and good thermal stability.

The thermal stability of aluminas has been improved by optimization of the synthesis procedure (e.g. sol–gel, co-precipitation, reverse micro emulsion). Doping with some additives such as alkaline-earth metals, rare-earth metals, silicon and phosphorus, or a combination of both, is a proper choice, but complicated procedures and rigid operation conditions augment the complexity

* Corresponding author. Tel.: +54 342 452 8062; fax: +54 342 453 1068.
E-mail address: usedran@fiq.unl.edu.ar (U. Sedran).

0920-5861/$ – see front matter © 2010 Elsevier B.V. All rights reserved.
doi:10.1016/j.cattod.2010.08.003

of the synthesis process and the associated costs [4]. Wang et al. [5] developed a novel and facile method for preparing thermostable γ-alumina as catalyst support through hydrolysis of phosphide aluminum, obtaining nanoparticles with a high surface area (285 m^2/g).

The atrane route has been developed as a new option in the synthesis of solid materials that could be directed to the synthesis of aluminum oxides for commercial catalytic applications. Among the derivatives of polyfunctional alcohols, one of the most common is tri-ethanolamine ($TEAH_3$). This reagent forms quelated complexes called atranes (i.e. complexes which include tri-ethanolamine-like ligand species) with a wide variety of metals (M) [6]. In this way, it is possible to generate a large variety of atranes from alkoxides or low-cost reagents (oxides or salts) by simply heating at ca. 130 °C the precursors in tri-ethanolamine.

The increasing demands to process heavier crudes and residual feedstocks, to control contaminants, and to maximize the yields of petrochemical raw materials, are the main issues imposing new trends in modern refineries [7]. These facts impact significantly on the main processes in refineries, such as the catalytic cracking of hydrocarbons (FCC), aimed at the conversion of low value, heavy hydrocarbon feedstocks into lighter, more valuable products such as liquefied petroleum gases, gasoline and diesel fuel. It is also a consequence that the formulation of FCC catalysts is shifting to high accessibility, resid or bottoms upgrading catalysts with active matrices and specific additives [8]. The matrix in a FCC catalyst provides the proper particle size and shape for the circulation of the catalyst particles in the unit, a heat sink to transport heat from the regenerator to the reactor, and a good contact between reactant molecules and the zeolite component [9]. The matrix could also be active and supply a pre-cracking activity for the very large molecules in the feedstock that cannot diffuse directly into the zeolite structure [10]. Indeed, aluminas are used as FCC catalyst active matrices [11].

It is the objective of this work to report the results of the characterization of aluminas that could be used as matrices in FCC catalysts. They were synthesized by the atrane route, using aluminum as the metal (M) in the atrane under various water/atrane complex relationships in the hydrothermal process. Their catalytic performances in the conversion of tri-isopropylbenzene, used as a test reactant for the measurement of the accessibility property in FCC catalysts [12], were assessed. The conventional sol–gel technique [13] was used to yield reference, comparative materials.

2. Materials and methods

The synthesis of the aluminum oxides was produced from the alumatrane, $Al[N(CH_2–CH_2–O)_3]$, atrane complex, designated as AlTEA, in two different ways. An aluminum source (aluminum tri-sec butoxide, Merck, 98%) was mixed with tri-ethanolamine (Sigma, 98%) at 120 °C with stirring to yield the AlTEA atrane complex, and then mixed with water under different proportions while adding 30% concentrated ammonia to achieve a pH value of 11 and produce the precipitation of the aluminum hydroxide. This product was subjected to hydrothermal treatment by heating at a rate of 10 °C/min to 200 °C and maintaining this temperature during 48 h. Samples were identified as "xx_ht", where xx indicates the molar relationship between water and AlTEA. Then the solid was washed and dried, and finally calcined at 700 °C during 4 h. In this way, four different samples were produced, according to conditions shown in Table 1. In one of the preparations (water/AlTEA relationship of 26), a fraction of the precipitated aluminum hydroxide was allowed to mature at room temperature during 48 h, and finally calcined at 700 °C during 4 h to yield a reference sample produced by the sol–gel method, named "26_sg".

Table 1
Molar water/AlTEA relationships used in the synthesis of the aluminas.

Sample	Water/AlTEA
9_ht	9
26_ht	26
52_ht	52
78_ht	78
26_sg	26

The various samples were subjected to X-ray diffraction analysis in a Rigaku–Geiger Mex diffractometer, using Cu-Kα1 1.5418 Å radiation in the 3°–60° 2θ angle range at 2°/min rate.

The ^{27}Al MAS-NMR analyses were performed in an Ultra Shield apparatus at 350 MHz, 30 min swapping time, 220 V source power.

Infrared spectra were collected in a Beckman spectrometer under the following conditions: Nichrom source, fast swapping rate, 12 min swapping time, 110 V power source, and double beam transmittance axis.

Picnometry studies were carried out with a LMS picnometer at 20 °C.

Specific surface areas were determined with the BET technique using nitrogen adsorption at 77 K in an AUTSORB-1c QUANTACHROME equipment. Solids were previously degassed at 473 K under a pressure of 10 mm Hg. Pore size distributions were assessed from the adsorption branch in the isotherms.

The evaluation of the catalytic performances of the various samples was performed in a laboratory CREC Riser Simulator reactor [14]. The reactor has a turbine on top of a chamber that holds the catalyst bed between porous metal plates. The turbine rotates at 7500 rpm, inducing a low pressure area in the upper central zone in the reactor that makes gases to re-circulate in the upwards direction through the chamber and fluidize the catalyst bed. When the reactor is at the desired experimental conditions, the reactant is fed with a syringe through an injection port and vaporizes instantly, thus setting the initial time. After the desired reaction time is attained, the gaseous mixture is evacuated immediately and products can be sent to analysis. Additional descriptive details can be found in, e.g. Passamonti et al. [15] and Al-Khattaf [16]. The experiments of conversion of 1,3,5-tri-isopropylbenzene (TIPB, Fluka 97%) were conducted at 500 °C, with a mass of catalyst of 0.4 g, catalyst to oil relationship (C/O) of 2.34 and reaction times of 12, 16, 20 and 30 s. Catalyst particles ranged from 8 to 180 μm. Mass balances (recovery) in the experiments were higher than 94% in all the cases. The products of the reaction were analyzed by conventional on-line capillary gas chromatography. Coke was determined by means of a temperature programmed oxidation procedure; carbon oxides from the combustion were transformed into methane and quantified with the help of a FID detector.

3. Results and discussion

3.1. Characterization of the aluminum oxy-hydroxides

Gel materials (aluminum oxy-hydroxides) were obtained after the moderate hydrothermal treatment at 200 °C in the synthesis procedure. The XRD analysis of these materials showed crystalline micro domains of the γ-AlOOH boehmite-type, that grew as a function of the water/AlTEA relationship used (see Fig. 1 with examples of uncalcined catalysts 9_ht and 78_ht, compared with a boehmite-type structure). This result is due to the amount of organic material trapped in the laminar network; in effect, the higher the amount of water in relation to AlTEA, the more ordered the mesostructures and the larger the crystalline micro domains [17].

The ^{27}Al MAS-NMR spectra of the aluminum oxy-hydroxides mesophases can be exemplified with that of the sample 26_ht

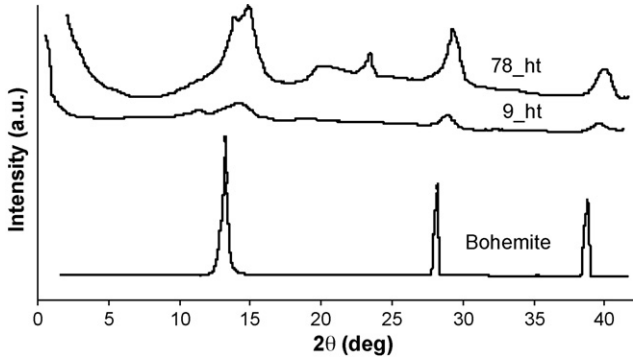

Fig. 1. XRD patterns of the uncalcined samples 9_ht and 78_ht, and boehmite-type structure.

Table 2
IR band assignments, sample 26_ht.

ν (cm^{-1})	Assignment
3295, 3090	OH (boehmite-type stretching)
2959, 2924, 2846	C–H (stretching)
1614	N–H (bending)
1467	C–H (symmetric bending)
1066	Al–O (boehmite)
727, 609, 470	Al–O–Al (boehmite)
1200	C–C (bending)
250–650	C–OH (out of plane flexion)

(see Fig. 2). Three signals can be seen at chemical shift δ values of 54, 33 and 6.5 ppm, their relative intensities being 1:1:10, that correspond to three different Al coordination environments: tetrahedral, pentacoordinated and octahedral, respectively [17,18]. The more intense signal corresponds to octahedral aluminum atoms, in consistency with the crystalline micro domains of the γ-AlOOH boehmite-type observed. The tetrahedral (δ = 54 ppm) and pentacoordinated (δ = 33 ppm) signals could belong to partially hydrolyzed aluminum atoms, and suggest that the boehmite micro domains are dispersed into an amorphous matrix [6].

Moreover, the bands observed in the IR spectra of the uncalcined samples shown in Fig. 3 can be attributed to vibrations that are typical of aluminum oxy-hydroxides, as indicated in Table 2. It can be seen that when the water/AlTEA relationship is increased, the bands tend to show a boehmite-type profile. Vibrations corresponding to the tri-ethanolamine organic portion can also be observed, such as those belonging to the C–C or C–H bonds in the ethyl groups, that can be linked or not to the aluminum in the organic–inorganic network [6].

Even though a hydrothermal treatment was performed, the organic material identified in the IR spectra, as well as the various coordination numbers for the aluminum atoms indicated by the NMR analysis of these mesostructured materials, suggest that the processes of hydrolysis and condensation of the $Al[N(CH_2–CH_2–O)_3]_2H_3$ complex in the aqueous medium is not complete. This is consistent with the alumatrane resistance to hydrolysis [18], although higher proportions of water in the mixture tend to favor it. Small amounts of water assist to start hydrolysis, but AlTEA excess slows down its rate, leading to incomplete hydrolysis and condensation [19]. If water is increased against AlTEA, the hydrolysis and condensation are accelerated, thus favoring a more robust inorganic network, with a higher trend to generate boehmite-type micro domains and to reduce the amorphous phases.

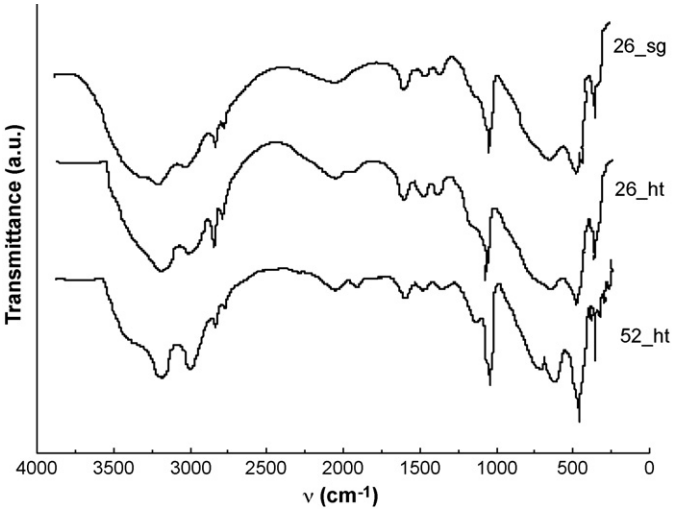

Fig. 3. IR spectra of uncalcined samples with different water/AlTEA relationships: 26_sg, 26_ht and 52_ht.

3.2. Characterization of the mesoporous aluminum oxides

The XRD studies of the samples after the calcination leading to mesoporous oxides showed an increase in the size of the γ-alumina micro domains, which can be associated to a higher order in the structure of the materials, linked to the increase in the water/AlTEA relationship in the synthesis (refer to Fig. 4), similarly to the observations with the uncalcined gels. The signals corresponding to the sample 26_sg are much less intense than those of the "xx_ht" samples.

The cell parameters of the γ-alumina phase characterized by XRD are a_o = 4.758 Å and c_o = 13.991 Å [20], with an fcc-type crystalline structure. Since it is a disordered phase that can be confused

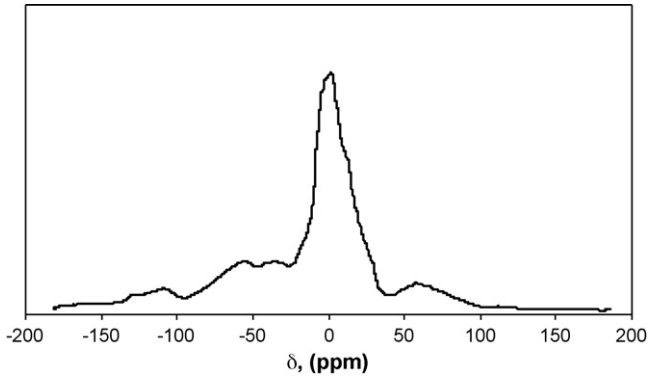

Fig. 2. ^{27}Al MAS-NMR spectrum of the uncalcined sample 26_ht.

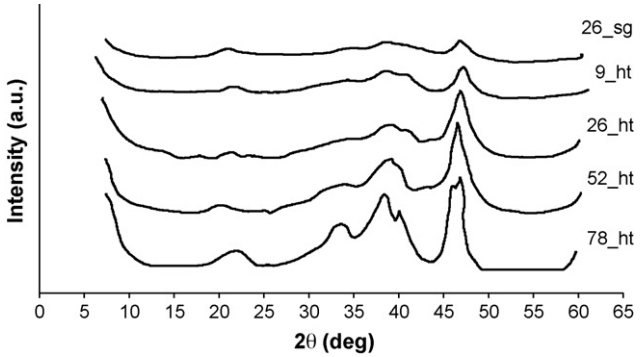

Fig. 4. XRD patterns of the calcined samples 26_sg, 9_ht, 26_ht, 52_ht and 78_ht.

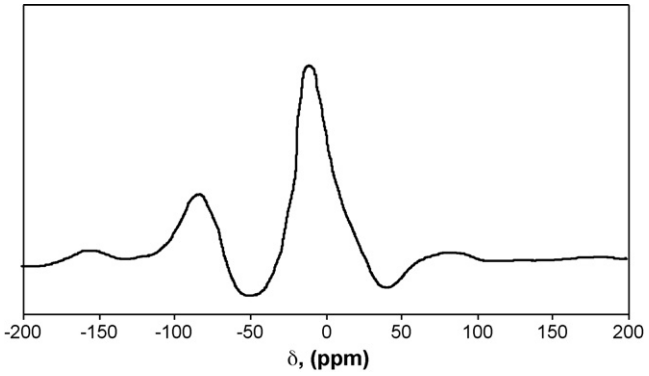

Fig. 5. ^{27}Al MAS-NMR spectrum of the calcined sample 26_ht.

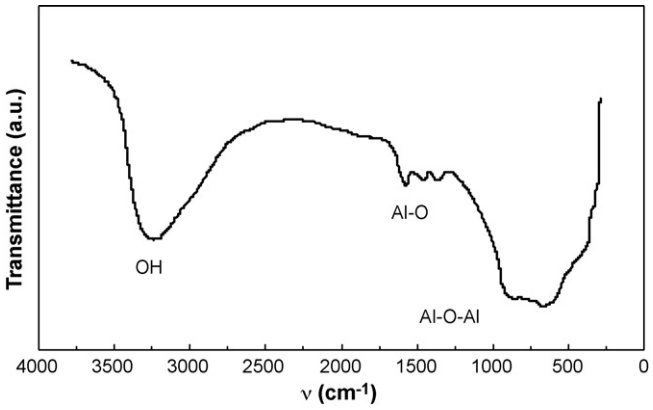

Fig. 6. IR spectrum of calcined sample 26_ht.

with an amorphous phase, it is difficult to determine it. However, most of the authors in the area suggest that it is close to an "inverse spinel", with an almost cubic unit cell having 32 oxygen atoms in an fcc array, the aluminum atoms being octahedrical [21]. In this case, the aluminum may substitute tetrahedrical Mg in the spinel.

The ^{27}Al MAS-NMR spectra of the oxides are exemplified in Fig. 5 with the case of the sample 26_ht showing two signals of chemical shift at $\delta = 79.8$ ppm and $\delta = 8.9$ ppm, which can be assigned to tetrahedral and octahedral aluminum atom environments, respectively. If compared to the uncalcined material (refer to Fig. 2), it can be seen that the peak corresponding to pentacoordinated aluminum is missing, thus implying a higher degree of order in the structures. The calcination process, then, increases the proportion of aluminum sites with octahedrical and tetrahedrical symmetry, particularly octahedral, in consistency with the formation of the γ-alumina phase. These tetrahedral aluminum sites may influence the acidic properties of the aluminas [21]. Similar profiles were observed in the other samples.

The comparison of the IR spectra of the calcined and uncalcined samples (refer to Figs. 3 and 6, case of sample 26_ht) shows that the bands corresponding to the organic matter due to the incomplete hydrolysis and condensation, distributed in the inorganic network in the mesostructured material, disappeared after calcination. The bands characteristic of the Al–O bonds and terminal OH groups, that can confer acidic properties to the oxide, can be observed.

The low angle XRD spectra of the samples 26_ht and 52_ht are shown in Fig. 7; they show broad peaks corresponding to, respectively, interplanar distances $d = 78 \pm 15$ Å and $d = 95 \pm 30$ Å, that are consistent with a "wormhole-like" pore structure [18]. The peak for the sample 26_ht is narrower, suggesting higher regularity in the pore size distribution. These evidences were also supported by TEM micrographs.

Table 3
Microdomain crystal size in the calcined samples.

Sample	Crystal size (Å)
9_ht	120
26_ht	152
52_ht	170
78_ht	200
26_sg	80

According to the IR and XRD observations, there exists a correspondence between the oxides and the mesostructured materials that in turn depends on the molar water/AlTEA relationships used in the synthesis. It can be concluded that higher proportions of water in relation to AlTEA in the synthesis increases the rate of hydrolysis and condensation, leading to the formation of crystalline micro domains with a boehmite-type structure distributed in an amorphous network where organic material is trapped [4]. Then, the calcination generates a porous oxide by means of the transformation of the boehmite-type micro domains into γ-alumina-type phases distributed in an amorphous matrix [22,23].

The size of the crystalline γ-alumina-type micro domains in the aluminas, as assessed with the Scherrer's equation also depends on the water/AlTEA relationship. Results shown in Table 3 reveals that the higher the water content, the larger the size, from about 120 Å in sample 9_ht to about 200 Å in sample 78_ht. This is consistent with the transformations from boehmite-type to γ-alumina-type structures observed in the synthesis [4,24]. On the other hand, the

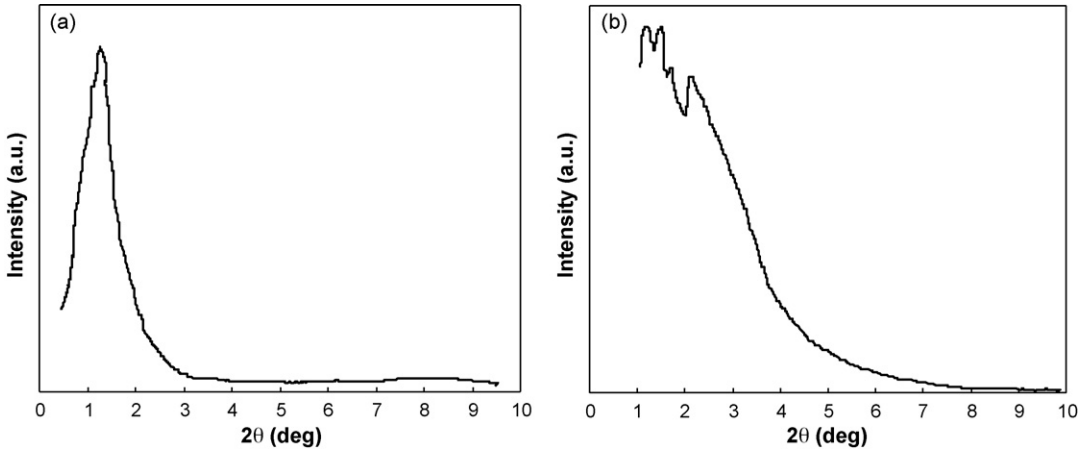

Fig. 7. Low angle XRD spectra of calcined samples: (a) 26_ht and (b) 52_ht.

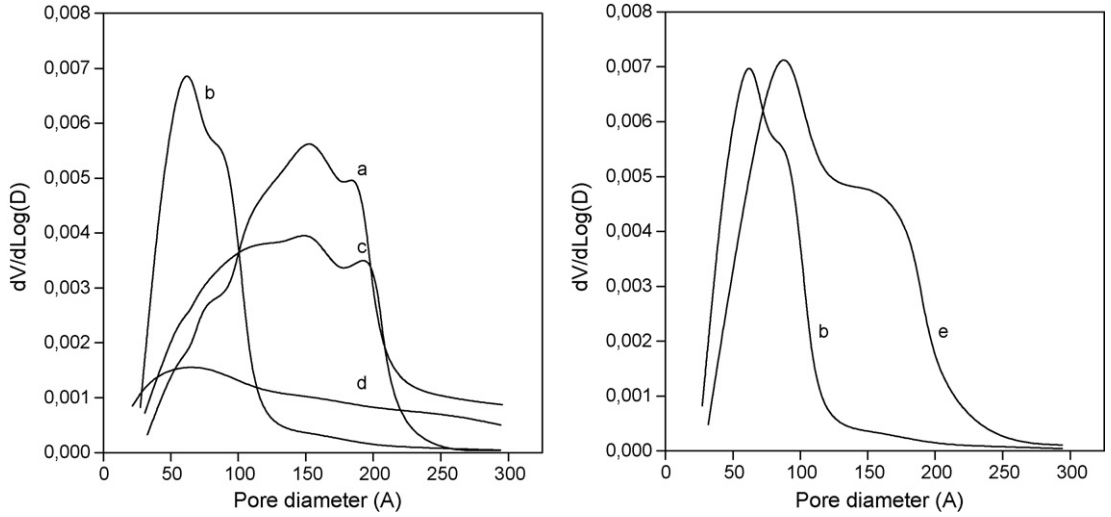

Fig. 8. (a) Pore size distibutions of the samples: (a) 9_ht, (b) 26_ht, (c) 52_ht and (d) 78_ht; (b) comparison between samples: (b) 26_ht and (e) 26_sg.

sample 26_sg (sol–gel method) showed a smaller crystal size of 80 Å.

The physical properties of the calcined samples are shown in Table 4. These properties of the aluminas are crucial in terms of their possible application as FCC catalyst matrices. It can be seen that the density of the calcined samples showed a clear trend as a function of the water/AlTEA relationship in the synthesis, increasing steadily with the water content. The specific surface area of the oxides ranged from about 150 to 275 m^2/g, without a clear trend as a function of the conditions in the synthesis. However, the pore size distributions were different, with average pore sizes in the 60–180 Å range. In effect, as shown in Fig. 8, the sample 26_ht showed a sharper, almost unimodal pore size distribution, while the other samples had pore sizes in a wide range. The sample synthesized with the sol–gel method (26_sg) showed the highest specific surface area, in the same range as the "xx_ht" samples. However, this oxide showed a wider distribution in the pore sizes as compared to the homologous sample 26_ht with the same water/AlTEA relationship in the hydrothermal method; this is consistent with a more important trapping of organic material in the inorganic–organic network during the maturing step in the direct sol–gel method, finally leading to a more dispersed pore system during the calcination step [25].

It can also be seen in Table 4 that the aluminas showed specific surface areas that may represent those of matrices in FCC catalysts of different types. Particularly for resid catalyst, it has been mentioned that, in general terms, they should have a mixture of meso- (about 60 Å mean pore size) and macropores (about 200–400 Å mean pore size) [26].

3.3. Assessment of the catalytic performance—accessibility

The conversion of TIPB over mesoporous materials can be used as a test reaction for the assessment of accessibility properties following a kinetic approach [12]. In this way, the simultaneous diffusion, adsorption and reaction of bulky molecules would be considered. The molecules of TIPB are bulky, with a kinetic diameter of 9.4 Å [27]. The expected lower activity of these aluminas as compared to compound FCC catalysts, allowed to perform the experiments of TIPB conversion at 500 °C, a temperature typical of many FCC units.

The most important products from the reaction, propylene (C3=), benzene (Bz), cumene (CUM), di-iso-propylbenzene (DIPB) and a TIPB isomer (C9Bz), indicated that simultaneous isomerization and series cracking reaction mechanisms prevailed. Also cadine isomers were observed. Typical yield curves are shown in Fig. 9 for the case of sample 26_sg, similar behaviors being observed in the other catalysts. The conversions observed at different reaction times are shown in Table 5, as well as the amount of coke on catalyst at the longest reaction time.

Table 4
Specific surface area, pore volume and density of the calcined samples.

Sample	Specific surface area (m^2/g)	Density (g/cm^3)	Pore volume (cm^3/g)
9_ht	216.7	2.31	0.741
26_ht	252.1	2.38	0.435
52_ht	202.2	2.41	0.580
78_ht	147.9	2.49	0.289
26_sg	274.4	2.39	0.748

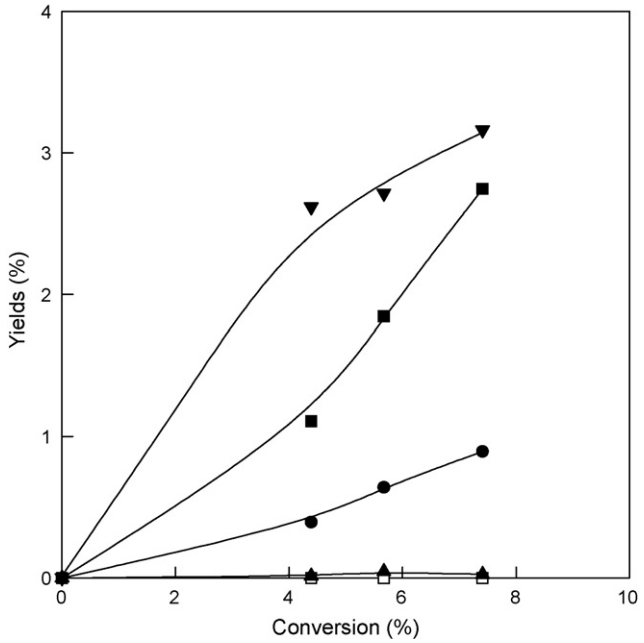

Fig. 9. Yield curves in TIPB conversion on sample 26_sg. Symbols: (●) C3=; (□) Bz; (▲) CUM; (■) DIPB; (▼) C9Bz.

Table 5
TIPB conversion (%) as a function of reaction time, coke on catalyst at 30 s, and apparent first order kinetic constant.

Reaction time (s)	Catalyst				
	9_ht	26_ht	52_ht	78_ht	26_sg
12	4.79	6.87	6.60	5.32	4.39
20	6.63	8.95	8.90	4.89	5.67
30	7.59	9.34	9.52	5.62	7.41
Coke at 30 s (%)	0.14	0.17	0.10	0.10	0.07
k ($\times 10^2$ cm^3/(g s))	0.35	0.46	0.47	0.28	0.34

There exists a specific index developed to evaluate the property of accessibility in FCC catalysts, namely the Albemarle accessibility index (AAI). The test measures the liquid phase diffusion of large molecules (asphalthenes) into the catalyst by means of an UV spectrometer, by tracking the relative concentration of the molecules that adsorb at certain wavelength as a function of time [28]. It can explain some facts of the catalytic performances; however, the experimental conditions used are far from those of the commercial process. Usual values for equilibrium FCC catalysts range from 0 (no accessibility) to 36 (very high accessibility); a higher accessibility would ensure a better performance in terms of higher gasoline yields and conversions and lower slurry yields. In previous works, the indexes observed in amorphous mesopores alumina matrices were from 29 to 45 [12], that is, close to the upper limit of applicability of the method.

The activities of the aluminas in the conversion of TIPB could also be defined by means of the apparent first order kinetic constants in a simple model representing the direct conversion of the reactant to products without catalyst deactivation. The apparent kinetic parameters from such a model included in Table 5 were assessed through a conventional least-square optimization method, fitting the experimental data (mass fraction of TIPB) to the model. The activities of these aluminas are similar, samples 26_ht and 52_ht being slightly more active. Moreover, considering the pore sizes in the various samples, the pore systems seem not to exert diffusion limitations. The activities observed are somewhat smaller than those of other aluminas under similar conditions [12] that averaged 0.95 cm^3/(g s), even though the physical properties are similar. It is to be noted that equilibrium commercial FCC catalysts, where Y zeolite is typically present at about 10–20%, are much more active than aluminas. In effect, their activities are more than 10 times higher than those of the alumina matrices.

4. Conclusions

Mesostructured aluminas can be synthesized following the atrane route, with aluminum tri-sec butoxide as the metal source mixed with tri-ethanolamine to yield the alumatrane complex. In the resulting uncalcined materials the amount of organic matter trapped in the inorganic matrix decreases as a function of the increasing molar relationship between water and AlTEA in the synthesis, because the higher proportion of water favors the hydrolysis and condensation of the $Al[N(CH_2–CH_2–O)_3]_2H_3$ complex. This is also the reason for the higher size of the crystalline micro domains of the γ-AlOOH boehmite-type as a function of the proportion of water. The calcination treatment induces the crystalline restructuration from boehmite-type to γ-alumina-type structures. In this way, the calcined mesoporous aluminas show an amorphous structure, with crystal micro domains of γ-alumina-type, which increase their size as a function of the amount of water in the starting mixtures. The specific surface areas are in the 150–275 m^2/g range and the average pore sizes in the 60–180 Å range. As compared to the conventional sol–gel method, the moderate hydrothermal treatment in the atrane synthesis route favors the release of trapped organic matter and the formation of initial boehmite-type micro domains; the resulting surface areas are similar, but the pore size distributions are sharper in the materials prepared with the atrane route.

The activities of the aluminas prepared by the atrane route, as indicated by the TIPB conversion, are somewhat smaller than those observed in conventional aluminas. The apparent kinetic parameters in a simple, first order model are similar, suggesting that accessibility limitations from the pore systems are not present. The properties shown by these aluminas synthesized by the atrane route indicate a preliminary appropriate condition for being used as FCC catalyst matrices.

Acknowledgements

This work was performed with the financial assistance of National University of Litoral, Secretary of Science and Technology (Santa Fe, Argentina) CAI+D 2005, Proj. 01-07; National Council for Scientific and Technical Research (CONICET) PIP 6285/05, and National Agency for Scientific and Technological Promotion PICT 2005 14-32930.

References

[1] L. Sicard, B. Lebeau, J. Patarin, F. Kolenda, Synthesis of mesostructured or mesoporous aluminas in the presence of surfactants. Comprehension of the mechanisms of formation, Oil Gas Sci. Technol. Rev. IFP 58 (2003) 557–569.
[2] R.K. Oberlander, Aluminas for catalysts—their preparation and properties, in: B.E. Leach (Ed.), Applied Industrial Catalysis, vol. 3, Academic Press, 1984, pp. 63–113.
[3] C. Lesaint, G. Kleppa, D. Arla, W. Glomm, G. Øye, Synthesis and characterization of mesoporous alumina materials with large pore size prepared by a double hydrolysis route, Micropor. Mesopor. Mater. 119 (2009) 245–251.
[4] A. Rabenau, The role of hydrothermal synthesis in preparative chemistry, Angew. Chem. Int. Ed. Engl. 24 (1985) 1026–1040.
[5] Y. Wang, J. Wang, M. Shen, W. Wang, Synthesis and properties of thermostable γ-alumina prepared by hydrolysis of phosphide aluminum, J. Alloys Compd. 467 (2009) 405–412.
[6] S. Cabrera, J. El Haskouri, J. Alamo, A. Beltrán, D. Beltrán, S. Mendioroz, M.D. Marcos, P. Amorós, Surfactant-assisted synthesis of mesoporous alumina showing continuously adjustable pore sizes, Adv. Mater. 5 (1999) 379–381.
[7] P. O'Connor, A. Hakuli, A. Humphries, J. Francis, Proc. Fifth South American Meeting on Catalytic Cracking, Maceió, Brazil, August 26–29, 2002, p. 25.
[8] K.Y. Yung, P. O'Conor, S.J. Yanik, K. Bruno, Catalytic solutions to new challenges in residue fluid catalytic cracking, Catal. Courier 53 (2003) a2.
[9] R. Von Ballmoos, C.T. Hayward, Matrix vs zeolite contributions to the acidity of fluid cracking catalysts, Stud. Surf. Sci. Catal. 65 (1991) 171–183.
[10] P. O'Connor, S.J. Yanik, Resid FCC operating regimens and catalyst selection, Stud. Surf. Sci. Catal. 100 (1996) 323–337.
[11] Y.-H. Lin, M.-H. Yang, Catalytic pyrolysis of polyolefin waste into valuable hydrocarbons, over reused catalyst from refinery FCC units, Appl. Catal. A: Gen. 328 (2007) 132–139.
[12] M. Falco, E. Morgado, N. Amadeo, U. Sedran, Accessibility in alumina matrices of FCC catalysts, Appl. Catal. A: Gen. 315 (2006) 29–34.
[13] M. Campanati, G. Fornasari, A. Vaccari, Fundamentals in the preparation of heterogeneous catalysts, Catal. Today 77 (2003) 299–314.
[14] H.I. de Lasa, U.S. Patent 5,102,628 (1992).
[15] F.J. Passamonti, G. de la Puente, U. Sedran, Reconversion of olefinic cuts from fluidized catalytic cracking naphthas, Ind. Eng. Chem. Res. 43 (2004) 1405–1410.
[16] S. Al-Khattaf, Xylenes reactions and diffusions in ZSM-5 zeolite based catalyst, Ind. Eng. Chem. Res. 46 (2007) 59–69.
[17] J. Livage, Sol–gel synthesis of heterogeneous catalysts from aqueous solutions, Catal. Today 41 (1998) 3–19.
[18] S. Cabrera, Chemistry of organizad media for obtaining mesoporous new aluminas, aluminosilicates and ALPOs with controlled pore sizes, Ph.D. Thesis, Universitat de Valencia, Spain, September 1999.
[19] R. Pujro, P. Crespo, P. Amoros, La ruta de los atranos en la síntesis de óxidos mixtos mesoporosos $Al_2Ti_xO_{3-2x}$, Rev. Bol. Quim. 24 (2007) 26–32.
[20] G. Lozano, E. Lozada, A. Guevara, Efecto de la descomposición del soporte sobre las estructuras superficiales de óxidos de Níquel y Molibdeno soportados en Óxidos mixtos TiO_2–Al_2O_3, Revista Mexicana de Ingeniería Química 5 (December (3)) (2006) 311–320 (Universidad Autónoma Metropilotana – Iztapalapa, México).
[21] G. Gutiérrez, Propiedades estructurales, dinámicas y electrónicas de Al_2O_3, Dissertation at the Physics Department, Faculty of Sciencies, University of Chile de Chile, May 20, 2005.

[22] D. Segal, Chemical synthesis of ceramic materials, J. Mater. Chem. 7 (1997) 1297–1305.
[23] S. Cabrera, J. El Haskouri, C. Guillem, J. Latorre, A. Beltrán-Porter, D. Beltrán-Porter, M.D. Marcos, P. Amoros, Generalised syntheses of ordered mesoporous oxides: the atrane route, Solid State Sci. 2 (2000) 405–420.
[24] F. Vaudry, S. Khodabandeh, M. Davis, Synthesis of pure alumina mesoporous materials, Chem. Mater. 8 (1996) 1451–1464.
[25] Q. Huo, D.I. Margolese, U. Ciesla, D.G. Demuth, P. Feng, T.E. Gier, P. Sieger, A. Firouzi, B.F. Chmelka, F. Schüth, G.D. Stucky, Organization of organic molecules with inorganic molecular species into nanocomposite biphase array, Chem. Mater. 6 (1994) 1176–1191.
[26] J.S. Magee, W.S. Letzsch, Fluid cracking catalyst performance and development, in: Proc. ACS Symposium Series, ACS, Washington, USA, 1994, p. 571.
[27] K. Ross, A. Liepold, H. Koch, W. Reschetilowski, Impact of accessibility and acidity on novel molecular sieves for catalytic cracking of hydrocarbons, Chem. Eng. Technol. 20 (1997) 326–332.
[28] A.K. Hakuli, P. Imhof, C.W. Kuehler, Understanding FCC catalyst architecture and accessibility, in: Proc. Akzo Nobel ECO-MAGIC Symposium, Noordwijk, The Netherlands, June 10–13, 2001 (F-4).